2015 IEEE 54th Annual Conference on Decision and Control (CDC)
December 15-18, 2015. Osaka, Japan

Lyapunov Stability Analysis of a Mosquito-Inspired Swarm Model

Daigo Shishika[1] and Derek A. Paley[2]

Abstract— **Self-propelled particle models have been used to study the collective behavior of animal groups such as fish schools and bird flocks, and these models have also been useful in designing control strategies for fleets of autonomous vehicles. In this paper, we construct a dynamical particle model inspired by mating swarms of wild mosquitoes. The model generates three different behaviors (swarming, velocity alignment, and pursuit) by switching the model parameters. Behaviors are generated by interaction forces based on springs and dampers. Previous studies of mosquito flight data suggest proximity in the velocity space, as well as the spatial distance, may determine the type of interaction. The stability properties of the velocity-alignment behavior, which generates intermittent parallel motion, and its effect on the success of the pursuit behavior are studied using Lyapunov analysis. The results presented in this paper may yield new understanding of the function of male-male interactions observed in mating swarms.**

I. Introduction

Self-propelled particle models are useful in modeling and analyzing collective behavior of animals. Couzin et al. [1] used a particle model to investigate the spatial dynamics of an animal group such as a fish school or bird flock; this model revealed the existence of major, group-level behavioral transitions related to minor changes in individual-level interactions. Scott and Leonard [2] studied a three-agent model involving a single pursuer (a bear) and two evaders (a mother caribou and her calf), and performed stability analysis on some equilibrium formations. Gazi and Passino [3] studied a general class of attraction/repulsion functions that can be used to achieve swarm aggregations; they presented stability analysis to characterize swarm cohesiveness, size, and motion.

Particle models are not only useful in investigating animal behaviors, but have also been used to design formation controls for multiple vehicles. For example, Leonard and Fiorelli [4] presented a framework for coordinated and distributed control of multiple autonomous vehicles using artificial potentials and virtual leaders. Paley and Leonard [5] showed the stability of the parallel and circular group motion presented in [1], and extended it to a control law for trajectory tracking. Olfati-Saber and Murray [6] presented a dynamic, graph-theoretic framework for flocking and used it to achieve obstacle avoidance. Gazi [7] considered a general model for vehicle dynamics and used sliding-mode control theory to track the motion of swarm members presented in [3].

This paper presents a particle model to investigate the collective behavior of animals, specifically the swarming behavior of insects such as mosquitoes or midges. Swarming insects are different from fish schools or bird flocks in the sense that their motion is not polarized. Nonetheless, swarms exhibit interesting features that have attracted research interest [8][9].

This study is inspired by the swarming behavior of malarial mosquitoes in the *Anopheles gambiae* species complex [10]. In our previous work, we observed cohesive oscillatory motion [11], as well as local interactions represented by intermittent parallel flight [12]. However, the pursuit behavior, which is one of the key aspects of a mating swarm, was not previously modeled. In order to accommodate pursuit, we extend the model presented in [12], while minimizing the overall complexity of the model. We further seek to use this model to investigate the possible role of intermittent parallel flight performed by the males in the swarm.

The contributions of this paper are (1) construction of a mosquito-inspired, dynamical particle model that generates swarming, velocity alignment, and pursuit behavior by switching parameters; (2) Lyapunov analysis of the weak stability of the velocity matching behavior, which is based on proximity in the velocity space; and (3) the study of the effect of velocity matching behavior on the success of pursuit behavior. This paper may yield new understanding of the function of male-male interactions observed in mating swarms, which could potentially be applied to control strategies for a multi-vehicle system.

Section II describes three behaviors observed in mosquito mating swarms in previous studies. Section III constructs a model that generates the three behaviors of male mosquitoes and discusses the connection to flight data. Section IV analyzes the Lyapunov stability of the velocity-matching behavior and studies the effect on pursuit. Section V summarizes the paper and ongoing and future work.

II. Background

The *Anopheles gambiae* species complex comprises the primary vectors of malaria in much of sub-Saharan Africa, and most of the mating in these species occurs when solitary females encounter swarms composed almost entirely of males [10]. One important area of investigation in the mating system of these malaria vectors is the nature and extent of male-male interactions in the swarm. Male-male interactions are explained by theories of lek-formation [13], including aggression or arena defense, collectively increased

[1]Daigo Shishika is a graduate student in the Department of Aerospace Engineering, University of Maryland, 20742 MD College Park, USA daigo.shishika@gmail.com

[2]Derek A. Paley is the Willis H. Young Jr. Associate Professor of Aerospace Engineering Education in the Department of Aerospace Engineering and the Institute for Systems Research, University of Maryland, 20742 MD College Park, USA dpaley@umd.edu

978-1-4799-7886-1/15/$31.00 ©2015 IEEE

signaling to females, and association with successful males. Another important question is the mechanism that leads to male-female coupling. Whether there is female evasion or selection is unknown. This section reviews several studies of the behavior of this malarial mosquito, which inspired the subsequent analysis.

A. Velocity Fluctuation

Butail et al. [11] obtained three-dimensional positions and velocities of swarming mosquitoes from stereoscopic video sequences and described the oscillatory motion of male mosquitoes in the swarm. Let $\mathbf{r}_i, \mathbf{v}_i$, and $\mathbf{a}_i$ be the position, velocity, and acceleration, respectively, of mosquito i with respect to an inertial point O, and let m denote the mass. Using the dynamic model of Okubo [14], the force on mosquito i was modeled as a linear combination of an external force $\mathbf{F}_i^{(\text{ext})}$, a drag force $\mathbf{F}_i^{(\text{drag})}$, and an interaction force $\mathbf{F}_i^{(\text{int})}$, i.e.,

$$m\mathbf{a}_i = \mathbf{F}_i^{(\text{ext})} + \mathbf{F}_i^{(\text{drag})} + \mathbf{F}_i^{(\text{int})}. \tag{1}$$

Velocity fluctuation was modeled as a damped oscillator whose frequency ω_0 and damping ratio ξ were gleaned from velocity-autocorrelation analysis of reconstructed flight data. The first two components in (1) resulted from a damped spring that connects each mosquito to the swarm centroid, assumed to be fixed in an inertial frame. That is,

$$\mathbf{F}_i^{(\text{ext})} + \mathbf{F}_i^{(\text{drag})} = -\operatorname{diag}\{\mathbf{k}\}\mathbf{r}_i - \operatorname{diag}\{\mathbf{b}\}\,(\mathbf{v}_i \cdot \hat{\mathbf{r}}_i)\,\hat{\mathbf{r}}_i, \tag{2}$$

where $\hat{\mathbf{r}}_i = \mathbf{r}_i / \|\mathbf{r}_i\|$, and the parameters $\mathbf{k}$ and $\mathbf{b}$ denote the three-dimensional spring and damping constants, respectively. Since the internal interaction force is unknown, white noise was used instead, i.e., $\mathbf{F}^{(\text{int})} = \mathbf{w}$. The noise intensity was also determined by the autocorrelation data analysis.

B. Velocity Alignment

Evidence for male-male interactions in mosquito swarms was provided in [11] using velocity disagreement between neighbors as a metric. In [12], we applied the unit-velocity cross correlation to further study the interaction between males in the swarm. Let $C_{ij}(t) \in [-1, 1]$ denote the unit-velocity cross correlation between the ith and jth mosquitoes at time t, and let m^* denote the lag value that maximizes the correlation value. The definition is

$$\begin{aligned} C_{ij}(t) &\triangleq \tilde{C}_{ij}(m^*, t) \\ &= \frac{1}{2}\Big(\tilde{r}_{ij}(m^*, t) + \tilde{r}_{ji}(-m^*, t)\Big), \quad \text{where} \\ \tilde{r}_{ij}(m, t) &= \frac{1}{T+1} \sum_{n=-\frac{T}{2}}^{\frac{T}{2}} \mathbf{v}_i(t+n+m) \cdot \mathbf{v}_j(t+n). \end{aligned}$$

The unit-velocity cross correlation measures the degree of interaction (if any) between two mosquitoes according to the alignment in their direction of motion (see Figure 1a). Analyses of the unit-velocity cross correlation led to two findings: (1) males form synchronized subgroups whose size and membership change rapidly; and (2) an interacting pair is likely to fly closer together than a non-interacting pair, but the velocity-matching interaction does not appear to be based on spatial proximity (see Figure 1b).

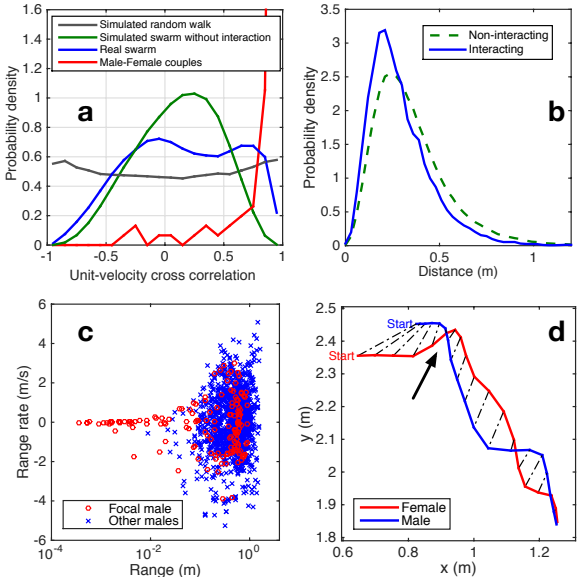

Fig. 1. Features of the flight patterns exhibited in mosquito mating swarms [10][11][12]. (a) Distribution of the unit-velocity cross correlation used to detect interactions represented by parallel flight. (b) Probability distribution of the distance between interacting and non-interacting pairs. (c) The range (i.e., the distance from a male to the female) and the range rate (i.e., the time derivative of the range) shown for focal male (i.e., successful in forming a mating couple with a female) and all other males. (d) An example of the trajectory in a coupling flight. The close encounter that appears to trigger the males's pursuit behavior is indicated by the arrow.

In [12], we constructed the following interaction force model represented by a velocity damper that connects each interacting pair:

$$\mathbf{F}_i^{(\text{int})} = \lambda \sum_{j \in \mathcal{S}} b^{\text{int}}\,(\mathbf{v}_{ji} \cdot \hat{\mathbf{r}}_{ji})\,\hat{\mathbf{r}}_{ji} + (1-\lambda)\mathbf{w}_i, \tag{3}$$

where $\lambda \in (0, 1]$ creates a convex combination of the damping force and the random force when mosquito i is in the interacting state. The topology of directed interaction was determined as follows: males interact if the disagreement in the direction of their motion is less than a specified threshold; one is picked randomly to be the follower for the duration of interaction (see [12] for details). Hence, the interaction is initiated based on the proximity in the unit-velocity space. This model showed a good agreement with the actual flight data in terms of the probability distribution of the unit-velocity cross correlation.

C. Coupling Flight

A female mosquito is attracted to the mating swarm and typically flies through it several times before coupling with a single male and leaving the swarm. Evidence for the role of pheromone in this behavior has been studied for a related species of mosquito [15]. The *Anopheles* female flies faster than the male, but the female slows down—and the male

speeds up—so their speeds match at the time of coupling. *Anopheles* are also known to synchronize harmonics of their wing-beat frequency during coupling flight [16].

The mechanism that triggers the male (or female) to transition from swarming to pursuit behavior is unknown, however, field data suggests that it may be related to spatial proximity. Figure 1c shows the proximity between the female and all other males, indicating that unsuccessful males are rarely as close to the female as the successful male. Figure 1d shows the trajectory of the male-female coupling flight. The space between the dashed lines increases after the close encounter with the female (shown by the arrow), indicating the acceleration of the male. These data suggest the possibility that the male's pursuit behavior is triggered by a close encounter with the female.

The forces (or, presumably, feedback behaviors) that govern pursuit are also unknown. Nonetheless, observations of motion from flight data (Figure 1d) suggest interactions in the coupling stage result from a damped-spring force.

III. Particle Model

The goal of this section is to add flexibility to the existing swarming models (see Section II), in order to accommodate, with minimal complexity, the following three behaviors in a single model: swarming, velocity-matching, and pursuit.

A. Force Model

Consider the following continuous-time, dynamical model of N identical, unit-mass particles subject to (planar) forces:

$$\mathbf{a}_i = \mathbf{F}_i^{(\text{space})} + \mathbf{F}_i^{(\text{align})} + \mathbf{F}_i^{(\text{ext})} \quad (i = 1, 2, ..., N), \tag{4}$$

where $\mathbf{F}_i^{(\text{space})}$ and $\mathbf{F}_i^{(\text{align})}$ are the spacing and alignment forces that arise from interactions, respectively, and $\mathbf{F}_i^{(\text{ext})}$ denotes all other external forces, including air resistance and random disturbances. One difference from prior models [11], [12], [14] is that here we divide the interaction force into two terms and combine the drag force and unknown disturbance into one term.

Let $\mathbf{r}_{ji} \triangleq \mathbf{r}_j - \mathbf{r}_i$ and $\mathbf{v}_{ji} \triangleq \mathbf{v}_j - \mathbf{v}_i$ denote the relative position and relative velocity, respectively, of particles i and j in an inertial frame. Let $Q_s^{(i)} = \{k | \, \|\mathbf{r}_{ki}\| \leq \rho_s\}$ denote the set of particles within the perceptual range $\rho_s > 0$ of the ith particle, and $Q_a^{(i)} = \{k | \, \|\mathbf{v}_{ki}\| \leq \rho_a, \ \|\mathbf{r}_{ki}\| \leq \rho_s\}$ denote the set of particles that are also within interaction range $\rho_a > 0$ in the velocity space. We model each force term as follows:

$$\mathbf{F}_i^{(\text{space})} = c \sum_{j \in Q_s^{(i)}} (1 - x_0/\|\mathbf{r}_{ji}\|)\, \mathbf{r}_{ji} \tag{5}$$

$$\mathbf{F}_i^{(\text{align})} = b \sum_{j \in Q_a^{(i)}} \mathbf{v}_{ji} \tag{6}$$

$$\mathbf{F}_i^{(\text{ext})} = -d\mathbf{v}_i + \mathbf{w}_i, \tag{7}$$

where $\mathbf{w}_i$ represents random noise, and c, x_0, b, and d are the spring, rest length, damping, and drag constants, respectively. Figure 2 illustrates the model parameters.

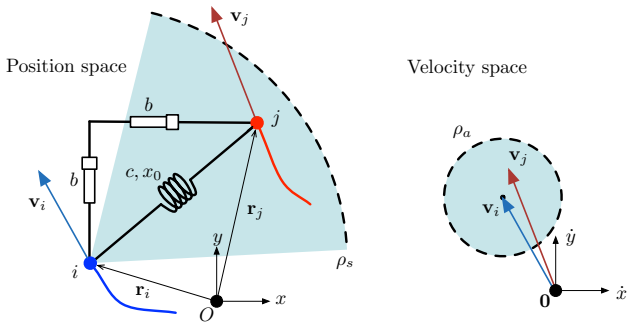

Fig. 2. Illustration of the model parameters. Particle i is in the velocity alignment state and $j \in Q_a^{(i)}$. The velocity damper produces a force in any direction.

In order to generate oscillatory motion, the spacing-force connects interacting particles as opposed to connecting each particle to a fixed point, as was considered previously [12] (see (2)). The previous model was valid for swarms that form above a fixed marker on the ground (this behavior is known to occur for only one of the two anopheline genetic types [10]). The new model accommodates swarming above a fixed point by adding a fixed, virtual particle. Noting that $\|\mathbf{r}_{ji}\| < x_0$ results in repulsion and $\|\mathbf{r}_{ji}\| > x_0$ in attraction, $\mathbf{F}^{(\text{space})}$ is a dynamical analogue of existing models with attraction and repulsion zones [1]. As mentioned in [3], each agent does not have to know the positions of all other agents in the swarm.

For the set $Q_a^{(i)}$, an annular region around the agent was considered in [1]. In [12], interactions were determined by proximity in the unit-velocity space (i.e., disagreement in the direction of motion), based on the idea that insects may be able to recognize other insects' motion and perform velocity matching only if their relative velocity is sufficiently small. The use of the dot product in [12] was convenient, because of the compatibility with the unit-velocity cross correlation. However, even when the distance is small in the unit-velocity space, the relative velocity can still be large if the speeds are sufficiently different. Using distance in the velocity space avoids this problem, and it is also convenient for the Lyapunov analysis presented in Section IV.

The relative velocity $\mathbf{v}_{ji}$ is generally not easy to measure (e.g., by sensing) for a moving agent if it has non-zero rotational velocity. However, mosquitoes do not rely heavily on yawing when they change their direction of motion [17]. In a planar problem, this condition makes the relative velocity in a body-fixed frame equivalent to the relative velocity in the inertial frame, which justifies the use of $\mathbf{v}_{ji}$ in the interaction model.

The alignment force $\mathbf{F}^{(\text{align})}$ was previously modeled as a damper that connects interacting particles [12]. While intuitively straightforward, its function as a velocity damper was limited because the force was constrained along the direction parallel to the line connecting those two particles. In the modified model (6), the alignment force is generated by two dampers that act independently in orthogonal directions,

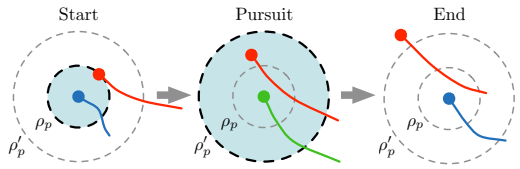

Fig. 3. The pursuit state from start to end. Blue and red represent the male and female, respectively. The male in the pursuit state is highlighted in green.

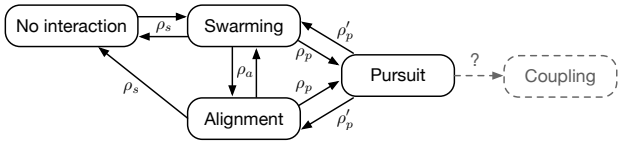

Fig. 4. State transition diagram for male mosquito. The parameters associated with the transition are shown. The male-female coupling phase is not shown.

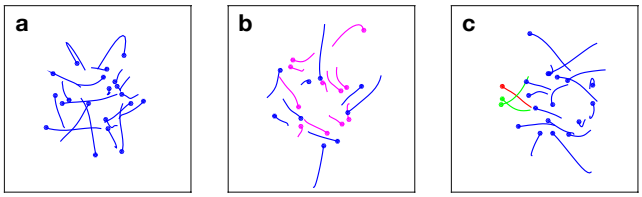

Fig. 5. (a) Swarming behavior. The alignment behavior is turned off by choosing ρ_a=0. (b) Velocity alignment behavior. Particles in the alignment state are highlighted in magenta. (c) Pursuit behavior. The red particle is the female and the green particles are in the pursuit state.

so that the force in the position space is arbitrary. This modification improves the velocity-matching function and also simplifies the model compared to the first term in (3).

B. Female Model and Pursuit

In order to consider pursuit behavior, we include one or more particles that represent M female mosquitoes, denoted $i = N+1, ..., N+M$. As mentioned in Section II, a female mosquito is attracted to the swarm and typically passes through it several times before coupling with a male. Therefore, we model the female as a particle attracted to its estimate of the centroid of the swarm. Let $\mathbf{r}_G$ denote the swarm centroid as estimated by the female: i.e., $\mathbf{r}_G = \frac{1}{n_f}\sum_{j\in\mathcal{N}_f}\mathbf{r}_j$, where $\mathcal{N}_f = \{k \mid \|\mathbf{r}_{kf}\| \le \rho_f\}$ denotes the set of males in the perceptual range ρ_f of the female and n_f denotes the number of elements in $\mathcal{N}_f$. Also let $\mathbf{r}_f$ denote the position of the female and $\mathbf{r}_{Gf} = \mathbf{r}_G - \mathbf{r}_f$. The spacing and external forces on the female are (there is no alignment force)

$$\mathbf{F}_f^{(\text{space})} = c_f\mathbf{r}_{Gf} \quad \text{and} \quad \mathbf{F}_f^{(\text{ext})} = -d\mathbf{v}_f + \mathbf{w}_f, \tag{8}$$

where c_f denotes the spring constant.

Inspired by observations of coupling flight, we impose the following rules on the male's pursuit behavior. A male starts pursuit when the female is within the range ρ_p, and continues as long as the female is in the range ρ'_p, where $\rho_p \le \rho'_p \le \rho_s$. All other interactions are ignored during pursuit, i.e., $Q_s^{(i)}$ and $Q_a^{(i)}$ are replaced by $Q_p^{(i)} = \{f\}$, where f denotes the index of the pursued female. Figure 3 summarizes the use of parameters ρ_p and ρ'_p.

C. Parameter Switching

In order to generate different behaviors, we switch the constants in the force model (5) and (6). Let $\emptyset$ denote an empty set. Particle i is in the

1) swarming state, if $Q_s^{(i)} \neq \emptyset$ and $Q_a^{(i)} = Q_p^{(i)} = \emptyset$;
2) alignment state, if $Q_a^{(i)} \neq \emptyset$ and $Q_p^{(i)} = \emptyset$; and
3) pursuit state, if $Q_p^{(i)} \neq \emptyset$.

By definition, the states are mutually exclusive, and the transitions between the states are summarized with the relevant parameters in Figure 4. The switching is summarized in Table I, and Figure 5 shows a simulation snapshot of each behavior generated by the model (4)—(7).

In the alignment behavior, the rest length of the spring is decreased relative to the swarming behavior (i.e., $x_a \le x_s$). This switch is inspired by the decreased distance between interacting pairs shown in Figure 1b. When the pursuit behavior is triggered by a close encounter with the female, the spring constant is increased relative to the swarming behavior (i.e., $c_p \ge c_s$).

IV. Lyapunov Stablity Analysis

One of the features in the collective behaviors of male mosquitoes is intermittent parallel flight that lasts for only a short duration of time. We hypothesize that weak stability of male-male interaction is key to the success in the mating. We first consider the cohesiveness of the swarm by looking at the total energy of the swarm. Then we analyze the Lyapunov stability of the velocity-alignment behavior. Finally, we consider how the velocity-matching behavior could be beneficial for subsequent pursuit.

A. Total Energy of the Swarm

As was studied in [3], the cohesiveness and size of the swarm are important considerations. Here, we use an energy function to show that a model swarm subject to interaction forces (5) and (6) is inherently stable. Consider the total energy of the system:

$$E = \frac{c_s}{2}\sum_{i,j\in Q_s}(\|\mathbf{r}_{ij}\| - x_s)^2 + \frac{c_s}{2}\sum_{i,j\in Q_a}(\|\mathbf{r}_{ij}\| - x_a)^2 + \frac{1}{2}\sum_i\|\mathbf{v}_i\|^2, \tag{9}$$

TABLE I
Parameter switching between three behavioral states.

	Swarming		Alignment		Pursuit
Spring constant (c)	c_s	$=$	c_s	$\le$	c_p
Rest length (x_0)	x_s	$\ge$	x_a	$\ge$	0
Damping constant (b)			b_a	$\le$	b_p

where the first summation is over all pairs in the swarming state, the second is over all pairs in the velocity-alignment state, and the third is over all particles. Assume that the magnitude of the random disturbance is bounded above as follows:

$$\|\mathbf{w}_i\| \leq w, \ \ \forall i \in \{1, .., N+M\} \tag{10}$$

Proposition 1: Consider a time interval $(t, t+dt)$ *in which the interaction topology remains constant. If* $w \simeq 0$*, then the total energy of the swarm* (9) *is non-increasing.*

Proof: The time derivative of the energy function is

$$\dot{E} = -b_a \sum_{i,j \in Q_a} \|\mathbf{v}_{ij}\|^2 - d \sum_i \|\mathbf{v}_i\|^2 + \sum_i (\mathbf{v}_i \cdot \mathbf{w}_i). \tag{11}$$

Therefore, if we ignore the random disturbance, $\dot{E}$ is negative semidefinite. ■

Noting that separation $\|\mathbf{r}_{ij}\|$ is bounded if E is bounded, *Proposition 1* shows that the swarm tends to remain cohesive rather than to disperse. If dt is sufficiently large, and $b_a \gg d$, the swarm will converge to a polarized motion in a static formation with $\mathbf{v}_{ij} = \mathbf{0}, \ \forall i, j$.

Proposition 1 notwithstanding, there are at least two ways for E to increase. One is from a change in the interaction topology. Let $U = c(\|\mathbf{r}_{ij}\| - x_0)^2/2$ denote the potential energy between i and j. Consider the case where particles i and j change from swarming to alignment behavior. The discontinuous change in E from this switching is

$$\begin{aligned} \Delta E &= U^{(\text{align})} - U^{(\text{swarm})} \\ &= c_s(x_s - x_a)\left(\|\mathbf{r}_{ij}\| - \frac{x_s + x_a}{2}\right). \end{aligned}$$

Hence, E increases if $\|\mathbf{r}_{ij}\| > (x_s + x_a)/2$ when the switching occurs, and decreases otherwise. (The opposite is true when the interaction switches from alignment to swarming.)

Another way for E to increase is by a random disturbance, which is clear from the last term in (11): i.e., $\dot{E}$ becomes positive or less negative if $\sum_i (\mathbf{v}_i \cdot \mathbf{w}_i) > 0$. When $\|\mathbf{v}_{ij}\|$ becomes smaller (resp. larger), the effect of the random disturbance becomes larger (resp. smaller) compared to the first term in (11). Hence, the energy of the system E fluctuates around a certain value that depends on the damping constant, the intensity of the random disturbance, and the interaction range parameters.

The idea of bounding $\|\mathbf{r}_{ij}\|$ and $\|\mathbf{v}_{ij}\|$ using an energy function is used to consider the stability of the swarm. In order to reduce complexity and make the problem tractable, in the following section we consider the stability property of a swarm with a specific initial condition.

B. Weak Stability of Velocity Alignment

Consider a swarm S consisting of $n < N$ particles and having an all-to-all interaction topology, i.e.,

$$\|\mathbf{r}_{ij}\| \leq \rho_s, \ \ \forall\, i, j \in S, \ \text{and} \tag{12}$$

$$\|\mathbf{v}_{ij}\| \leq \rho_a, \ \ \forall\, i, j \in S. \tag{13}$$

Note that all-to-all interactions occur here among all particles traveling in approximately the same direction. (The more general case in which the interaction is not all-to-all is the subject of ongoing work.) The question is whether the conditions (12) and (13) remain true for future time or not. The following two lemmas give the conditions that trap the particles in the all-to-all alignment, which in fact may be undesirable for mating success.

Lemma 1: Consider a set of n *particles with initial conditions satisfying* (12) *and* (13)*. The all-to-all alignment is stable (i.e.,* (13) *is true* $\forall\, t > 0$*) if* (12) *is true* $\forall\, t > 0$*, and*

$$(nb_a + d)\rho_a > nc_s\rho_s + 2w. \tag{14}$$

Proof: The Lyapunov function candidate $V = \frac{1}{2}\sum_{i,j \in S_a} \|\mathbf{v}_{ij}\|^2$ is not useful since (for $n > 3$) one or more of the terms in the summation can increase and violate the condition (13), while the overall V is decreasing. Therefore, consider pairwise stability with the Lyapunov function candidate

$$V_{(i,j)} = \frac{1}{2}\|\mathbf{v}_{ji}\|^2. \tag{15}$$

There are $\frac{n(n-1)}{2}$ of these functions. However, without loss of generality, we investigate the stability of a single pair $(i, j) = (1, 2)$ and generalize it to all other pairs. Let $\mathbf{\Delta}_{ji} = \mathbf{F}_j^{(\text{space})} - \mathbf{F}_i^{(\text{space})} + \mathbf{w}_j - \mathbf{w}_i$, denote the difference in the spacing and random forces acting on the ith and jth particles. We have

$$\begin{aligned} \dot{V}_{(1,2)} &= \mathbf{a}_{21} \cdot \mathbf{v}_{21} \\ &= \left[b_a \sum_{j \in S}(\mathbf{v}_{j2} - \mathbf{v}_{j1}) - d(\mathbf{v}_2 - \mathbf{v}_1) + \mathbf{\Delta}_{21}\right] \cdot \mathbf{v}_{21} \\ &= [-(nb_a + d)\mathbf{v}_{21} + \mathbf{\Delta}_{21}] \cdot \mathbf{v}_{21} \\ &\leq -\left(nb_a + d - \frac{a}{2}\right)\|\mathbf{v}_{21}\|^2 + \frac{1}{2a}\|\mathbf{\Delta}_{21}\|^2 \end{aligned}$$

where $a > 0$. Using the concept of ultimate boundedness [18], $\mathbf{v}_{21}$ remains in the interior of a ball with radius ρ_a centered at $\mathbf{0}$ if

$$\begin{aligned} &-\left(b_a + d - \frac{a}{2}\right)\rho_a^2 + \frac{1}{2a}\|\mathbf{\Delta}_{21}\|^2 < 0 \\ &\Leftrightarrow \|\mathbf{\Delta}_{21}\|^2 < 2a\left(nb_a + d - \frac{a}{2}\right)\rho_a^2 \\ &\Leftarrow \|\mathbf{\Delta}_{21}\| < (nb_a + d)\,\rho_a. \end{aligned}$$

One can also show that $\|\mathbf{\Delta}_{21}\| < nc_s\rho_s + 2w$, which completes the proof. ■

Lemma 1 shows that the strength of the velocity-matching interaction in terms of its robustness to the other forces becomes stronger with larger perception range ρ_a, drag constant d, and damping constant b_a. As the group size n increases, the effect of d and w becomes smaller.

Lemma 2: Consider a set of n *particles with initial conditions satisfying* (12) *and* (13)*. Let* $x_a' = x_a + 2w/nc_s$*. Assume* $x_a \ll \rho_s$*. The particles remain cohesive (i.e.,* (12) *is true* $\forall\ t > 0$*) if* (13) *is true* $\forall\ t > 0$*, and the following*

conditions are satisfied:

$$K \triangleq (\rho_s - x'_a)^2 - \frac{1}{c_s}\rho_a^2 > 0, \tag{16}$$

$$\textit{and} \quad \|\mathbf{r}_{ij}(0)\| \leq x'_a + \sqrt{K}, \ \ \forall\, i,j \in S_a. \tag{17}$$

Proof: Let $\mathbf{\Delta}_{21} \triangleq \mathbf{w}_2 - \mathbf{w}_1$. Since we want to bound the separation between two particles, consider the worst case where the disturbance is always acting in the direction that increases the separation. That is, suppose

$$\mathbf{\Delta}_{21} = 2w\frac{\mathbf{r}_{21}}{\|\mathbf{r}_{21}\|}.$$

Under the assumption $x_a \ll \rho_s$, one can show that this disturbance effectively changes the rest length from x_a to x'_a.

Now, consider the Lyapunov function

$$V = \frac{c_s}{2}(\|\mathbf{r}_{21}\| - x'_a)^2 + \frac{1}{2}\|\mathbf{v}_{21}\|^2.$$

Since V is non-increasing (proof omitted for page constraints), we have the following

$$\frac{c_s}{2}(\|\mathbf{r}_{21}(t)\| - x'_a)^2 \leq V(t) \leq \frac{c_s}{2}(\|\mathbf{r}_{21}(0)\| - x'_a)^2 + \frac{1}{2}\rho_a^2.$$

Hence, $\|\mathbf{r}_{21}(t)\| < \rho_s, \ \forall\ t > 0$ is guaranteed if the initial separation $\mathbf{r}_{21}(0)$ satisfies (17). Condition (16) ensures the existence of such $\mathbf{r}_{21}(0)$. ■

Lemma 2 shows that the strength of cohesion becomes stronger with a larger perception range and spring constant, and also that the particles must be initially close together.

Combining *Lemma 1* and *2*, cohesion and velocity alignment guarantee one another. In addition, conditions (14) and (16) can be combined to specify the right balance between the spacing and alignment force, which establishes the following proposition.

Proposition 2: Consider a set of n particles with the initial conditions satisfying (12)*,* (13)*, and* (17)*. Assume $x_a \ll \rho_s$. The all-to-all alignment is stable if*

$$\frac{nc_s}{nb_a + d}\rho_s + 2w < \rho_a < \sqrt{c_s}(\rho_s - \frac{2w}{nc_s}). \tag{18}$$

Moreover, if we assume $d \simeq 0$ and $w \simeq 0$, the condition reduces to

$$c_s\rho_s < b_a\rho_a < b_a\sqrt{c_s}\rho_s. \tag{19}$$

Staying in the alignment state by satisfying the conditions given in *Proposition 2* may be desirable in some cases (e.g., a formation control of vehicles). However, since we hypothesize that the intermittent alignment behavior is important, we want to see how the all-to-all interaction can be broken.

Unfortunately, the converse of *Proposition 2* is not true: i.e., we do not know whether the all-to-all interaction will be broken or not when (18) is violated. This point is clear if we look at the term $\mathbf{\Delta}_{21} \cdot \mathbf{v}_{21}$ in $\dot{V}_{(1,2)}$ in the proof of *Lemma 1*. Depending on the angle between $\mathbf{\Delta}_{21}$ and $\mathbf{v}_{21}$, the sign of $\dot{V}_{(1,2)}$ can change.

Violation of (18) potentially breaks the all-to-all alignment by increasing either the relative velocity or the separation between the particles in the group. The only control parameters that the particle chooses are the damping constant b_a and the spring constant c_s. Thus, with the right choice of b_a and c_s, the particle will exhibit parallel flights that are sufficiently weak so as to last only for a short duration.

C. Effect of Alignment Behavior on Successful Pursuit

The velocity-matching behavior affects a male's success in pursuit, using the following definition:

Definition 1: Pursuit of duration $T > 0$ is successful if $\delta t = t_{end} - t_{start} > T$, where t_{start} is the time when $\|\mathbf{r}_{fi}\|$ enters the range ρ_p and t_{end} is the time it leaves the range $\rho_{p'}$.

Note that T is typically much larger than the time it takes for a female to accidentally pass through the perceptual region of a male, i.e., $T \gg (\rho_p + \rho'_p)/\|\mathbf{v}_f\|$. Because the female's behavior is unknown, and because we are interested in the male's pursuit behavior, we define pursuit to be successful if a male stays close to the female. We now show that the chance of this success may be increased by the male's alignment behavior.

Proposition 3: Consider the pursuit behavior of male i and female f. Let $v_T = (\rho'_p - \rho_p)/T$. Pursuit of duration T is successful if

$$(b_p + d)v_T > c_f\rho_f + 2w, \ \ \textit{and} \tag{20}$$

$$\|\mathbf{v}_{fi}(t_{start})\| < v_T. \tag{21}$$

Proof: Following the proof of *Lemma 1*, (20) and (21) guarantees $\|\mathbf{v}_{fi}(t)\| < v_T$, $\forall t > t_{start}$. Then, the shortest time for f to leave the range ρ'_p of i is bounded below by

$$\min\{\delta t\} > (\rho'_p - \rho_p)/v_T > T,$$

which completes the proof. ■

The direct contribution of the velocity alignment term $\mathbf{F}^{(\text{align})}$ is seen in (20); i.e., condition (20) is satisfied if the damping constant b_p is sufficiently large. However, the more important effect is that the condition (21) is more likely to be satisfied if $\|\mathbf{v}_{fi}(t_{start})\|$ is made small by the velocity-alignment behavior prior to the start of the pursuit behavior.

The following result provides conditions that guarantee the success of pursuit of any duration. Consider the Lyapunov function candidate

$$V_P = \frac{1}{2}\|\mathbf{r}_{fi}\|^2 + \frac{1}{2c_p}\|\mathbf{v}_{fi}\|^2. \tag{22}$$

Proposition 4: Pursuit is stable (i.e., $\|\mathbf{r}_{fi}\| < \rho'_p$, $\forall\ t > t_{start}$) if the following are true:

$$c_f\rho_f + 2w \ < \ (b_p + d)\|\mathbf{v}_{fi}\|, \ \ \textit{and} \tag{23}$$

$$\|\mathbf{v}_{fi}(t_{start})\| \ < \ \sqrt{c_p\left(\rho'^2_p - \rho_p^2\right)}. \tag{24}$$

Proof: Let $\mathbf{\Delta}_{fi} = \mathbf{F}_f^{(\text{space})} + \mathbf{w}_f - \mathbf{w}_i$. Then we have

$$\begin{aligned} c_p\dot{V}_P &= c_p\mathbf{v}_{fi}\cdot\mathbf{r}_{fi} + \mathbf{a}_{fi}\cdot\mathbf{v}_{fi} \\ &= c_p\mathbf{v}_{fi}\cdot\mathbf{r}_{fi} + [-(b_p+d)\mathbf{v}_{fi} - c_p\mathbf{r}_{fi} + \mathbf{\Delta}_{fi}]\cdot\mathbf{v}_{fi} \\ &= -(b_p+d)\|\mathbf{v}_{fi}\|^2 + \mathbf{\Delta}_{fi}\cdot\mathbf{v}_{fi}. \end{aligned}$$

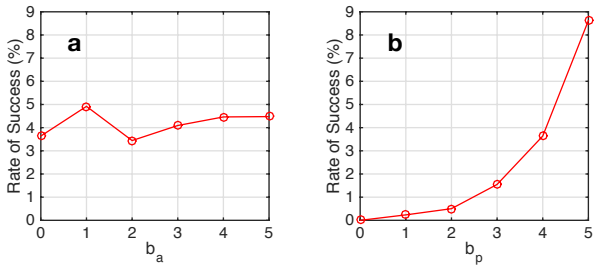

Fig. 6. The effect of velocity damping on the success of pursuit behavior. (a) The effect of parameter b_a, while $b_p = 4$ is held fixed. (b) The effect of parameter b_p, while $b_a = 0$ is held fixed.

Following the proof of *Lemma 1*, one can show that (23) guarantees $\dot{V}_P < 0$, which gives the bound $V_P(t) < V_P(t_{start})$ for all $t > t_{start}$. Also, from (22) the distance between f and i is bounded by $\|\mathbf{r}_{fi}\| \leq \sqrt{2V_P(t)}$. Noting that $\|\mathbf{r}_{fi}(t_{start})\| = \rho_p$, (24) implies that

$$V_P(0) < \frac{1}{2}\rho_p^2 + \frac{1}{2c_p} c_p \left(\rho_p'^2 - \rho_p^2\right),$$
$$2V_P(t) < 2V_P(0) < \rho_p'^2.$$

Hence the distance never exceeds the limit ρ_p'. ■

Condition (23) is strong since the right-hand side can be arbitrarily small. However, even if the condition is violated occasionally, the result of *Proposition* 4 remains true as long as $V_P(t)$ stays less than its initial value $V_P(t_{start})$. The conditions (23) and (24) also suggest direct effect of b_p and the indirect effect of b_a, respectively. These effects are highlighted by the numerical results shown in Figure 6. The success rate is calculated by dividing the total number of successes of duration $T = 1.2(s)$ by the total number of close encounters; i.e., incidents with $\delta t < T$. The simulation parameters are $N = 10, \rho_s = 0.5, \rho_p = 0.05, \rho_p' = 0.1, \rho_a = 0.1, c_s = 5, c_p = 15, c_f = 4, x_s = 0.3, x_a = 0.1$.

Figure 6a shows the indirect effect of velocity alignment (i.e., the potential decrease in $\|\mathbf{v}_{fi}(t_{start})\|$) by changing the value of b_a while $b_p = 4$ is held fixed. The success rate increases slightly with the value of b_a from 0 to 1. For larger b_a, the particles converge to polarized motion and their mobility is decreased, which may be a reason for the drop in the success rate. This result also shows the benefit of swarming as compared to a polarized formation flight. Figure 6b shows the direct effect of velocity alignment in the pursuit stage by varying the value of b_p. The effect is clearer due to a stronger interaction force in the pursuit state.

V. Conclusion

We present a dynamic particle model inspired by the mating swarms of *Anopheles gambiae*, which exhibit swarming, velocity alignment, and pursuit behaviors. Switching model parameters generates these behavioral states. The interaction topologies are inspired by flight data and prior observational studies. Lyapunov analysis shows that velocity-alignment behavior may improve the success rate of pursuit by decreasing the relative velocity prior to the onset of pursuit. Therefore, velocity matching may be performed in order to increase the success in mating. In ongoing work, we are refining the model of female behavior as well as considering the application of the model to the control of swarms of autonomous vehicles.

Acknowledgment

The authors would like to acknowledge valuable discussions with Nicholas Manoukis, Sachit Butail and Frank Lagor related to this work.

References

[1] I.D. Couzin, J. Krause, R. James, G.D. Ruxton, and N.R. Franks. Collective memory and spatial sorting in animal groups. *Journal of theoretical biology*, 218:1–11, 2002.

[2] W. Scott and N.E. Leonard. Pursuit, herding and evasion: A three-agent model of caribou predation. *American Control Conference*, (1):2984–2989, 2013.

[3] V. Gazi and K.M. Passino. A class of attraction/repulsion functions for stable swarm aggregations. *Proceedings of the 41st IEEE Conference on Decision and Control, 2002.*, 3(18):1567–1579, 2002.

[4] N.E. Leonard and E. Fiorelli. Virtual leaders, artificial potentials and coordinated control of groups. *Proceedings of the 40th IEEE Conference on Decision and Control (Cat. No.01CH37228)*, 3, 2001.

[5] D. Paley, N.E. Leonard, and R. Sepulchre. Collective motion: bistability and trajectory tracking. *2004 43rd IEEE Conference on Decision and Control (CDC) (IEEE Cat. No.04CH37601)*, 2(3):1932–1937, 2004.

[6] R. Olfati-Saber and R.M. Murray. Flocking with Obstacle Avoidance : Cooperation with Limited Information in Mobile Networks. *IEEE Conference on Decision and Control (CDC)*, (December):1–27, 2003.

[7] V. Gazi. Swarm aggregations using artificial potentials and sliding-mode control. *IEEE Transactions on Robotics*, 21:1208–1214, 2005.

[8] A. Attanasi, A. Cavagna, L. Del Castello, I. Giardina, S. Melillo, L. Parisi, O. Pohl, B. Rossaro, E. Shen, E. Silvestri, and M. Viale. Collective Behaviour without Collective Order in Wild Swarms of Midges. *PLoS Computational Biology*, 10(7):1–10, 2014.

[9] J.G. Puckett, D.H. Kelley, and N.T. Ouellette. Searching for effective forces in laboratory insect swarms. *Scientific reports*, 4:4766, 2014.

[10] N. C. Manoukis, A. Diabate, A. Abdoulaye, M. Diallo, A. Dao, A. S. Yaro, José M C Ribeiro, and Tovi Lehmann. Structure and dynamics of male swarms of Anopheles gambiae. *Journal of medical entomology*, 46(2):227–235, 2009.

[11] S. Butail, N. Manoukis, and M. Diallo. The Dance of Male Anopheles gambiae in Wild Mating Swarms. *Journal of Medical Entomology*, 50(3):552–559, 2013.

[12] D. Shishika, N.C. Manoukis, S. Butail, and D.A. Paley. Male motion coordination in anopheline mating swarms. *Scientific reports*, pages 1–7, 2014.

[13] B.M. Beehler and M.S. Foster. Hotshots, Hotspots, and Female Preference in the Organization of Lek Mating Systems. *The American Naturalist*, 131(2):203, 1988.

[14] A. Okubo. Dynamical aspects of animal grouping: swarms, schools, flocks, and herds. *Advances in biophysics*, 1986.

[15] M. Cabrera and K. Jaffe. An aggregation pheromone modulates lekking behavior in the vector mosquito Aedes aegypti (Diptera: Culicidae). *Journal of the American Mosquito Control Association*, 23(1):1–10, 2007.

[16] C. Pennetier, B. Warren, K. R. Dabiré, I. J. Russell, and G. Gibson. "Singing on the wing" as a mechanism for species recognition in the malarial mosquito Anopheles gambiae. *Current biology : CB*, 20(2):131–6, January 2010.

[17] S.M. Iams. *Characterizing Mosquito Flight Using Measurement and Simulation*. PhD thesis, 2014.

[18] H.K. Khalil and J.W. Grizzle. *Nonlinear Systems*. Upper Saddle River: Prentice hall, 2002.